

# Non-invasive assessment of hepatic iron stores by MRI

Y Gandon, D Olivié, D Guyader, C Aubé, F Oberti, V Sebille, Y Deugnier

## Summary

**Background** MRI has been proposed for non-invasive detection and quantification of liver iron content, but has not been validated as a reproducible and sensitive method, especially in patients with mild iron overload. We aimed to assess the accuracy of a simple, rapid, and easy to implement MRI procedure to detect and quantify hepatic iron stores.

**Methods** Of 191 patients recruited, 17 were excluded and 174 studied, 139 in a study group and 35 in a validation group. All patients underwent both percutaneous liver biopsy with biochemical assessment of hepatic iron concentration (B-HIC) and MRI of the liver with various gradient-recalled-echo (GRE) sequences obtained with a 1.5 T magnet. Correlation between liver to muscle (L/M) signal intensity ratio and liver iron concentration was calculated. An algorithm to calculate magnetic resonance hepatic iron concentration (MR-HIC) was developed with data from the study group and then applied to the validation group.

**Findings** A highly T2-weighted GRE sequence was most sensitive, with 89% sensitivity and 80% specificity in the validation group, with an L/M ratio below 0.88. This threshold allowed us to detect all clinically relevant liver iron overload greater than 60  $\mu\text{mol/g}$  (normal value  $<36 \mu\text{mol/g}$ ). With other sequences, an L/M ratio less than 1 was highly specific ( $>87\%$ ) for raised hepatic iron concentration. With respect to B-HIC range analysed (3–375  $\mu\text{mol/g}$ ), mean difference and 95% CI between B-HIC and MR-HIC were quite similar for study and validation groups (0.8  $\mu\text{mol/g}$  [–6.3 to 7.9] and –2.1  $\mu\text{mol/g}$  [–12.9 to 8.9], respectively).

**Interpretation** MRI is a rapid, non-invasive, and cost effective technique that could limit use of liver biopsy to assess liver iron content. Our MR-HIC algorithm is designed to be used on various magnetic resonance machines.

*Lancet* 2004; **363**: 357–62

See Commentary page 341

**Fédération d'Imagerie Médicale** (Prof Y Gandon MD, D Olivié MD), **Service des Maladies du Foie** (Prof D Guyader MD, Prof Y Deugnier MD), and **Centre d'Investigation Clinique** (V Sebille PhD, Prof Y Deugnier), **CHU Pontchaillou, Rennes, France;** and **Département de Radiologie** (C Aubé MD) and **Service de Gastro-entérologie** (F Oberti MD), **CHU, Angers, France**

**Correspondence to:** Prof Yves Gandon, Fédération d'Imagerie Médicale, Hôpital Pontchaillou, 35033 Rennes, France (e-mail: yves.gandon@chu-rennes.fr)

## Introduction

Iron excess, even when mild, is increasingly regarded as an important cofactor in the morbidity attributed to many disorders, including cancer,<sup>1</sup> cardiovascular diseases,<sup>2</sup> arthritis,<sup>3</sup> chronic liver disease,<sup>4</sup> and various states characterised by insulin resistance.<sup>5</sup> These putative widespread effects of iron probably account for why more and more patients are presently referred to hepatology and haematology clinics for assessment of body iron stores and discussion of iron removal by phlebotomy.<sup>6</sup> Assessment of body iron stores by measurement of serum ferritin concentrations has poor specificity.<sup>7</sup> The most reliable method to calculate body iron stores is histochemical or biochemical assessment of iron in a liver biopsy specimen.<sup>8</sup>

Because liver biopsy is an invasive procedure that should be restricted to management of liver disease, attempts have been made to use imaging to detect and quantify hepatic iron content. However, iron deposition is not detectable at ultrasound examination, hyperdensity on CT scan is not specific for iron and can be masked by associated steatosis,<sup>9,10</sup> and the SQUID (superconducting quantum interference) device is not in widespread use.<sup>11</sup> Because of the paramagnetic properties of iron, magnetic resonance signal diminishes in liver as iron concentration increases. Gradient-recalled-echo (GRE) techniques—more sensitive to field inhomogeneities induced by paramagnetic substances than spin-echo sequences—have been suggested to quantify liver iron excess.<sup>12–14</sup> This sensitivity makes MRI the most accurate routine imaging procedure to assess hepatic iron content, but, surprisingly, the technique is rarely used in management of patients with suspected iron overload, which is probably attributable to an absence of multicentric studies assessing reproducibility of MRI in this setting.

We aimed to assess the accuracy of a simple, rapid, and easy to implement MRI procedure in detection and quantification of hepatic iron stores, especially in patients with slight iron overload.

## Patients and methods

### Patients

During a 32-month period (March 1996, to October, 1998), all patients who were referred to two of us (YD or DG) and were scheduled to undergo liver biopsy at the Liver Unit, Rennes, France, for either suspicion of hepatic iron overload or management of chronic hepatitis C, were asked to undergo MRI for assessment of hepatic iron stores and offered biochemical determination of hepatic iron concentration from their liver biopsy specimen. These patients formed the study group. We did an identical study in consecutive patients admitted to the Liver Unit, Angers, France, and these patients comprised the validation group.

All included patients gave written informed consent to participate. The protocol for both studies was approved by the ethics committee of CHU Pontchaillou, Rennes.

## Procedures

### Data acquisition

With ultrasound guidance, we obtained a biopsy sample of the right lobe of the liver with a 16 gauge needle (Hepafix 16G, Braun, Melsingen, Germany). We measured fibrosis with a 5-grade scale, ranging from 0 (no fibrosis) to 4 (cirrhosis).<sup>15</sup> We assessed hepatic steatosis by determining the percentage of fatty hepatocytes. Using the Barry and Sherlock method,<sup>8</sup> we calculated biochemical hepatic iron concentration (B-HIC). We defined hepatic iron overload as B-HIC greater than 35  $\mu\text{mol/g}$  (dry liver).

We did magnetic resonance studies on a Signa unit (GE Medical Systems, Milwaukee, WI, USA) operating at a field strength of 1.5 T. To avoid signal depth fall-off, we obtained breath-hold sequences with a body coil, with a bandwidth of 12.5 KHz,  $256 \times 128$  matrix, field of view of 40 cm, and slice thickness of 10 mm. To calculate the liver to muscle (L/M) ratio for every sequence, we acquired five axial GRE sequences of the liver, with a repetition time of 120 ms. We defined variables that progressively enhanced sensitivity to iron overload.<sup>12</sup> A typical T1-weighted sequence with an in-phase echo time of 4 ms and a 90° pulse angle was followed by four sequences with a 20° pulse angle and in-phase echo times ranging from 4 to 21 ms, to progressively increase T2-weighting (table 1). Every sequence had an acquisition time of 15 s.

For every sequence, we measured liver signal intensity in three operator-defined regions of interest defined on the same image and drawn on the external part of the right hepatic lobe, with a workstation (Advantage Windows; GE Medical Systems, Milwaukee, WI, USA). These regions contained at least 100 pixels and avoided inclusion of vessels or artifacts. To calculate muscle signal intensity, we did the same procedure by placing two regions of interest on right and left paraspinal muscles, on the same transverse sections as those used to measure liver signal intensity, and avoided inclusion of intermuscular fat. We calculated the L/M ratio by dividing mean liver signal intensity by mean muscle signal intensity. Measurements were done by two radiologists independent of the study. We used the first set of measurements—done by an experienced radiologist—for the main statistical analysis; the second set, done separately by a resident, was used to test the effect of image choice and placement of region of interest to assess interobserver variability.

We established the detection threshold for every magnetic resonance sequence and examined diagnostic accuracy of L/M ratios for diagnosis of hepatic iron overload.

We defined, for every sequence, the saturation threshold—ie, the minimum value of L/M (L/Mmin), just above the noise level, corresponding to the maximum B-HIC (B-HICmax) that could be assessed by the sequence. We relied on findings of previous studies showing that, for a given magnetic resonance sequence, the relation between amplification of hepatic iron stores and decline of L/M ratio remained linear only up to a certain minimum ratio.<sup>12,16</sup>

	Acronym	TR (ms)	TE (ms)	PA (°)
T1 weighted GRE sequence	GRE T1	120	4	90
PD weighted GRE sequence	GRE PD	120	4	20
T2 weighted GRE sequence	GRE T2	120	9	20
T2+ weighted GRE sequence	GRE T2+	120	14	20
T2++ weighted GRE sequence	GRE T2++	120	21	20

TR=repetition time. TE=echo time. PA=pulse angle. PD=proton density.

Table 1: Magnetic resonance gradient echo sequences

Group	L/M threshold	Sensitivity (95% CI)	Specificity (95% CI)	Area	
GRE T1	S	1.35	74% (64–82)	86% (72–95)	0.85
	S+V	1	47% (38–57)	100% (78–100)	0.81
GRE PD	S	1.23	74% (64–82)	95% (84–99)	0.84
	S+V	1	48% (38–57)	97% (88–100)	0.83
GRE T2	S	1.22	90% (82–95)	95% (84–99)	0.94
	S+V	1	71% (62–79)	95% (86–99)	0.93
GRE T2+	S	1.07	90% (82–95)	98% (88–100)	0.96
	S+V	1	86% (78–92)	95% (86–99)	0.95
GRE T2++	S	0.88	93% (85–97)	98% (88–100)	0.97
	V	0.88	89% (67–98)	80% (52–95)	0.94
	S+V	1	95% (89–98)	88% (77–95)	0.96

S=study group. V=validation group. Area=area under the ROC curve. Optimum L/M threshold was determined with ROC curves, with the best compromise between sensitivity and specificity on the study group and apply to the validation group using the most sensitive MR sequence. L/M threshold of 1 was also tested on the combination of the two groups.

Table 2: Sensitivity and specificity of L/M ratio for every sequence

On the basis of these results, we developed software to automatically estimate hepatic iron concentration. The software algorithm first selected the most sensitive sequence giving an L/M ratio greater than its own saturation threshold—ie, L/Mmin—and then calculated hepatic iron concentration (MR-HIC) with the corresponding correlation curve of B-HIC as a function of the ratio, excluding values less than L/Mmin.

To make the optimum acquisition protocol and to establish the best possible sequence combination allowing maximum detection and accurate quantification of liver iron content, the number of sequences used by the software to calculate MR-HIC was progressively reduced from five to two. We compared values of MR-HIC and B-HIC for the various combinations.

In patients in the validation group, magnetic resonance measurements to calculate L/M ratio were made with a Signa 1.5 T magnetic resonance unit (GE Medical Systems) by one radiologist (CA). The saturation threshold and algorithm defined by study group data were applied to L/M data derived from this validation group. We compared the values of MR-HIC and B-HIC between groups.

### Statistical analysis

We used the area under the receiver operating characteristic (ROC) curve to assess the MRI algorithm. For every sequence, we used the following procedure to define L/Mmin and to derive the corresponding MR-HIC value: (1) diminishing L/M ratios were introduced step by step; (2) the correlation coefficient ( $r$ ) between L/M ratio and B-HIC was calculated at every step and  $r$  was derived; (3) inclusion of L/M ratio was stopped as soon as  $r$  reached its maximum value, with the last value introduced corresponding to L/Mmin. We then calculated MR-HIC on the basis of a regression of L/M ratio on B-HIC.

We compared MR-HIC and B-HIC with the Bland and Altman statistical method for phase of optimisation of the

	L/Mmin	Number of patients	$r$ (95% CI)	B-HICmax
GRE T1	0.13	129	0.92 (0.85–0.99)	375
GRE PD	0.14	127	0.91 (0.83–0.98)	343
GRE T2	0.22	108	0.89 (0.80–0.98)	163
GRE T2+	0.2	97	0.88 (0.78–0.98)	136
GRE T2++	0.2	91	0.87 (0.77–0.97)	102

GRE T1=T1-weighted GRE sequence. GRE PD=proton density weighted GRE sequence. GRE T2=T2-weighted GRE sequence. GRE T2+ and GRE T2++=highly T2-weighted GRE sequence.

Table 3: Correlation between L/M ratio and B-HIC with determination of B-HICmax according to every magnetic resonance sequence

acquisition protocol and for the validation group.<sup>17</sup> This comparison was applied to two subgroups of patients: one with B-HIC less than B-HIC<sub>max</sub> (375  $\mu\text{mol/g}$ ) of the less sensitive sequence, to obtain a global correlation but excluding patients with major iron overload for whom a precise quantification is not possible by MRI; and one of patients with B-HIC less than 100  $\mu\text{mol/g}$ —ie, about three times the upper limit of normal—to compare results in patients with slight iron overload. We also used the Bland and Altman method to assess interobserver variability. Results were expressed as mean difference with 95% CIs.

We did all analyses with Statview 5 (SAS Institute, Cary, NC USA) and MedCalc (MedCalc Software, Mariakerke, Belgium).

### Role of the funding source

The sponsor of the study had no role in study design, data collection, data analysis, data interpretation, or writing of the report.

### Results

149 patients were enrolled into the study group and 42 into the validation group. Mean time between liver biopsy and MRI examination was 8.2 days (SD 23; range 0–194). No patient had phlebotomy or abnormal bleeding between liver biopsy and MRI. Total facility time per patient was about 15 min, including turnover time between patients. B-HIC and MR-HIC were not assessable in 11 and six patients, respectively, because of biopsy failure ( $n=1$ ), small size of biopsy sample ( $n=10$ ), metallic implants ( $n=3$ ), claustrophobia ( $n=2$ ), and cancellation of MRI appointment ( $n=1$ ). The study and validation groups finally consisted of 139 and 35 patients, respectively.

Of 139 patients in the study group, 45 (27 men) had normal B-HIC values and 94 (77 men) presented with enhanced B-HIC ranging from 36 to 709  $\mu\text{mol/g}$  (mean 172  $\mu\text{mol/g}$  [SD 148]). 19 (13%) patients had cirrhosis. Steatosis grade was greater than 30% in 25 patients.

As shown in table 2, the highest T2-weighted GRE sequence (GRE T2++) was the most sensitive. With an L/M threshold of 0.88, there were seven false negative patients, whose B-HIC ranged from 36 to 56  $\mu\text{mol/g}$ , and one false positive case, with a B-HIC of 30  $\mu\text{mol/g}$ . With a threshold of L/M of 1, there were four false positive patients with the most sensitive sequence (specificity 93%), no false positives with the T1-weighted sequence, and one false positive case with other sequences (specificity 97%).

A significant correlation between L/M decrease and B-HIC increase was noted whatever the magnetic resonance sequence studied ( $p<0.0001$ ; table 3). On the basis of the procedure to calculate L/M<sub>min</sub> and B-HIC<sub>max</sub>, which was used to establish the saturation threshold for every sequence (figures 1 and 2), the most and least sensitive sequences were noted to be operating up to a B-HIC<sub>max</sub> of 102  $\mu\text{mol/g}$  and 375  $\mu\text{mol/g}$ , respectively (table 3). Two points, both corresponding to patients with cirrhosis, were judged too discordant and were

excluded from this analysis step (points 1 and 2 in figure 3), but all patients below the saturation threshold (B-HIC <375  $\mu\text{mol/g}$ ,  $n=129$ ) were taken into account in further steps.

Comparison of B-HIC and MR-HIC gave a mean difference of 0.8  $\mu\text{mol/g}$  (95% CI –6.3 to 7.9). When patients with steatosis grade above 30% were excluded ( $n=105$ ), mean difference did not vary (–0.2 [95% CI –8.8 to 8.4]). When patients with cirrhosis were excluded ( $n=114$ ), this difference slightly increased but 95% CI fell (2.4 [–2.8 to 6.8]). When selecting patients with slight iron overload ( $n=87$ ; B-HIC <100  $\mu\text{mol/g}$ ), mean difference was unchanged but 95% CI declined (–0.7; [95% CI –2.7 to 4.1]). A mean difference of MR-HIC of 2.2  $\mu\text{mol/g}$  (95% CI –0.5 to 4.5) was recorded between the two radiologists.

With the same algorithm, but using four instead of five magnetic resonance sequences, the mean difference and 95% CI did not change between B-HIC and MR-HIC (data not shown). When using three sequences, only a combination of two of three T2 sequences (T2, T2+, or T2++) and the proton density sequence did not alter the mean difference and 95% CI. With only two sequences, the best result was noted by combination of proton density and T2++ sequences (mean difference –2.7 [95% CI –15.2 to 11.4]).

Of the 35 patients in the validation group, 16 (12 men) had no overload and 19 (16 men) had an abnormal increase of B-HIC, ranging from 38 to 348  $\mu\text{mol/g}$  (mean 122  $\mu\text{mol/g}$  [SD 74]). 20 patients (57%) had cirrhosis. Steatosis grade was more than 30% in six patients.

One very discordant false positive result in a young woman (point 3 in figure 3) in this group was regarded as

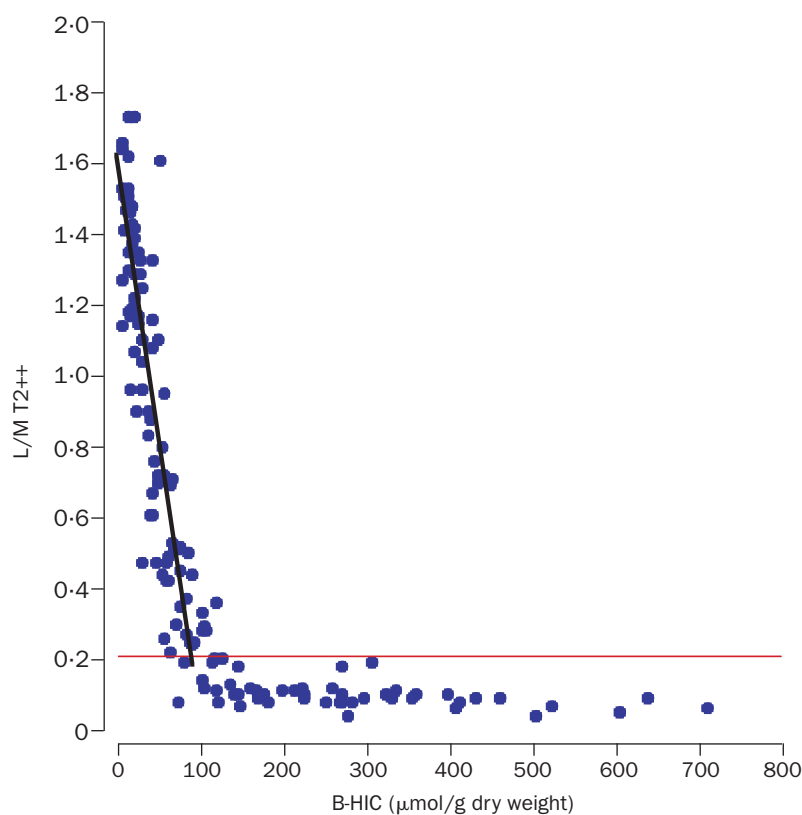


**Figure 1: Determination of saturation threshold of most sensitive sequence (GRE T2++)**

Correlation between B-HIC and L/M ratio with GRE T2++ sequence (L/M T2++). Saturation threshold (horizontal line) was defined by considering maximum of  $r$  coefficient when introducing, step by step, diminishing values of L/M T2++.

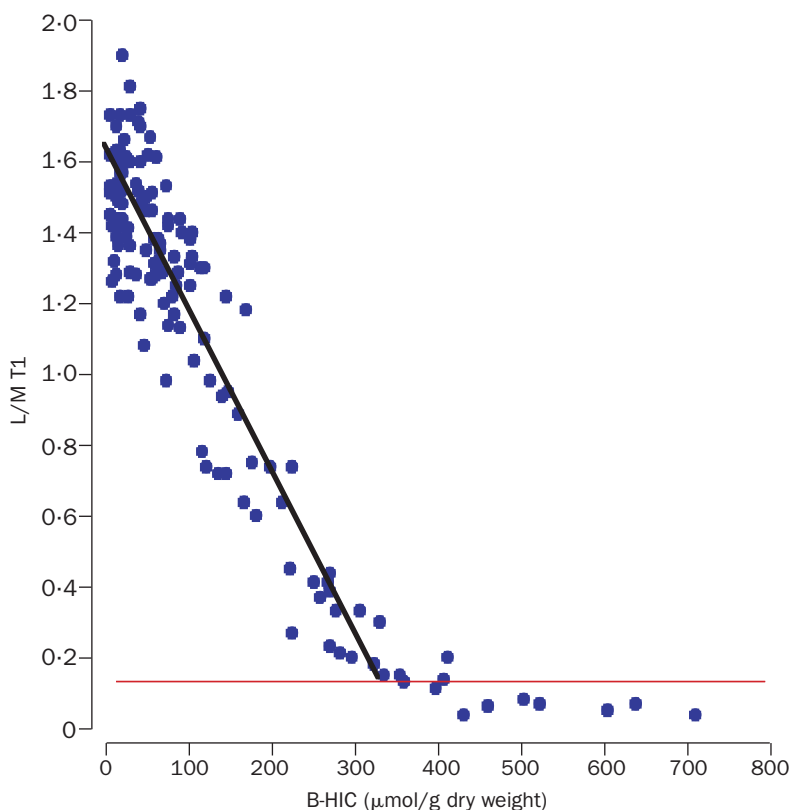


Figure 2: **Determination of saturation threshold of the less sensitive sequence (GRE T1)**

Correlation between B-HIC and L/M ratio with GRE T1 sequence (L/M T1). Saturation threshold (horizontal line) was defined by considering maximum of  $r$  coefficient when introducing, step by step, diminishing values of L/M T1.

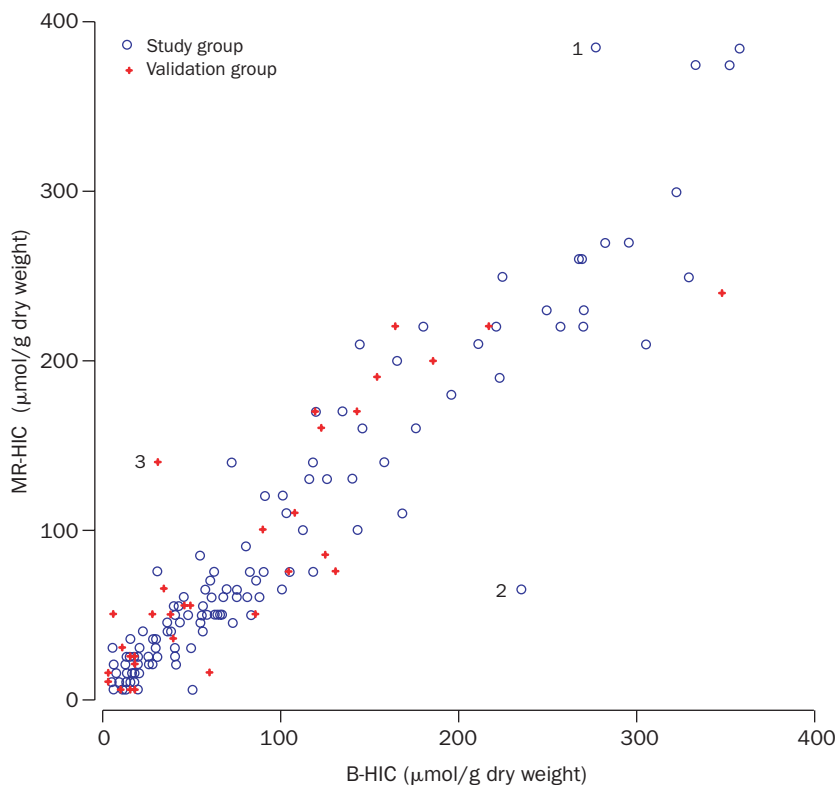


Figure 3: **MR-HIC versus B-HIC for study and validation groups**

Point 1 and 2, corresponding to patients with cirrhosis, were excluded for algorithm determination. Point 3 was a discordant result attributed to B-HIC error.

an error of biochemical assessment of liver iron content on the basis of the following arguments: age 19 years, serum iron concentration  $35 \mu\text{mol/L}$  (normal value  $<27 \mu\text{mol/L}$ ), transferrin saturation 105% (normal value  $<45\%$ ), serum ferritin concentration  $285 \mu\text{g/L}$  (normal value  $<150 \mu\text{g/L}$ ), C282Y homozygosity, and iron overload confirmed on semiquantitative assessment of liver iron by histology with a total iron score of 12/60. This patient was excluded from the statistical analysis.

With the detection threshold defined in the study group (L/M 0.88 on GRE T2++), there were three false positive and two false negative patients in the validation group (B-HIC 39 and  $60 \mu\text{mol/g}$ , respectively), giving 89% sensitivity and 80% specificity. With a threshold of L/M of 1, specificity was 87% for T2 and T2+ sequence and 100% for proton density and T1-weighted sequences. Mean difference (95% CI) between MR-HIC and B-HIC was similar to that for the study group for all patients included in the statistical analysis ( $n=34$ ;  $-2.1 \mu\text{mol/g}$  [ $-12.9$  to  $8.9$ ]) and for those with slight iron overload (B-HIC  $<100 \mu\text{mol/g}$ ;  $n=22$ ;  $-3.5 \mu\text{mol/g}$  [ $-12.1$  to  $5.1$ ]).

## Discussion

We have shown that MRI with GRE sequences on a 1.5 T magnet is a non-invasive alternative method for assessment of liver iron overload and quantification of hepatic iron concentration, from  $60 \mu\text{mol/g}$  to about ten times the upper limit of normal ( $375 \mu\text{mol/g}$ ).

Liver iron overload leads to a decline in liver magnetic resonance signal because of T2-shortening related to the paramagnetic properties of iron stored within the liver.<sup>18</sup> Unfortunately, magnetic resonance signal is dependent on multiple acquisition variables, and cannot be directly correlated to hepatic iron concentration. Thus, comparative quantitative data need to be extracted, either to determine absolute T2 (or T2 star) relaxation time<sup>12,19-21</sup> or to calculate ratios of signal intensities such as liver to noise,<sup>12,14</sup> liver to fat,<sup>12</sup> or liver to muscle.<sup>12,13,20,22</sup> Theoretically, T2 star calculated from one breath-hold multiecho GRE sequence is the best method to measure iron paramagnetic effects. However, this type of sequence is not implemented on all magnetic resonance devices. Liver to noise ratio has been proposed to serve as a reference to quantify significant iron overload at 1.5 T.<sup>14</sup> Findings of an experimental study have also established that with a 4.7 T magnet, the liver to noise ratio was slightly

better correlated to liver iron concentration than was the liver to muscle ratio.<sup>23</sup> However, in clinical practice, the main aim is to be able to detect and quantify a slight increase of liver iron overload in patients with a large range of bodyweights. A slight change in repetition time, field of view, or slice thickness can greatly alter the liver to noise ratio but only slightly the liver to muscle ratio. Moreover, significant variations of liver to noise ratio are seen from one MRI facility to another, even if machines are of the same type, which precludes standardisation of this index.<sup>14</sup>

Taking into account our previous experience,<sup>12</sup> and because our aim was to define a widely applicable protocol with minimum intermachine variations, we selected muscle to compare with liver. One major advantage of this choice is that liver signal is usually more intense than muscle, thus a slight decline in liver signal can be easily detected by simple visual comparison. An L/M ratio less than 1 is highly indicative of raised hepatic iron with most sequences, except the highly T2-weighted gradient echo sequence, for which the best specificity and sensitivity were obtained with an L/M ratio of 0.9. With this highly sensitive sequence, MRI identifies all liver iron overload greater than 60  $\mu\text{mol/g}$ , which is, in practice, a sufficient threshold. However, this protocol is incompatible with the phased-array multicoil, which is routinely used to investigate the liver, and needs a switch to the body coil.

Most patients with hepatic iron overload, irrespective of its cause, present with hepatic iron concentration within the range 60–375  $\mu\text{mol/g}$ . The high level of sensitivity of our method, by comparison with previous magnetic resonance findings, is attributable to use of a high field magnetic resonance unit, which amplifies the magnetic effect of iron.<sup>12,13</sup> This finding was previously suggested but not proven because the number of controls was fewer than seven.<sup>14,24</sup>

Good correlation was reported between MRI and biochemical assessment of iron overload. On the whole, presence of liver fibrosis did not affect the accuracy of our technique. However, outlier points corresponded to patients with cirrhosis, a disorder in which iron deposition is usually heterogeneous and biochemical hepatic iron concentration can vary greatly from one nodule to another, as shown in surgically removed liver samples.<sup>25</sup> MRI can examine transverse sections of the entire liver, and region of interest signal intensity measurements average larger volumes of tissue compared with liver biopsy samples. In accordance with other results,<sup>14</sup> this finding could suggest that, in patients with cirrhosis, overall assessment of hepatic iron concentration would be even more accurate than biopsy when done with MRI.

In our series, we did not record any effect of steatosis on iron quantification. This result was expected, since the fatty liver signal is increased only on T1-weighted images. In our algorithm, these images are used only when more sensitive sequences—including proton density sequence, which has the same sensitivity as T1-weighted sequence—are saturated by major overload. On GRE T2-weighted images, steatosis does not greatly modify magnetic resonance liver signal, since selected echo times are in-phase. In case of presence of fat and water in the same pixel, a relative loss of signal intensity occurs with opposed-phase GRE images.<sup>26,27</sup>

Assessment of hepatic iron concentration by our magnetic resonance algorithm had good interobserver reproducibility and was accurate with the same magnetic resonance unit operating at 1.5 T, although the proportion of patients with cirrhosis was greater in the validation group than in the study group (57% vs 16%).

This magnetic resonance technique has been successfully applied to several 0.5 T devices, a 1 T unit,<sup>28</sup> and a 1.5 T magnet.<sup>29</sup>

The procedure we propose has several advantages over liver biopsy, representing a non-invasive and safe technique that can be performed quickly. Unlike liver biopsy, it does not require preoperative biochemical and echographic assessment nor admission, thus it is much less costly and easily accepted by patients.<sup>14</sup> In this study, 5% of core specimens were too small to allow B-HIC measurement, whereas only 3% of patients had a failed magnetic resonance study.

Use of our calculation algorithm (available at <http://www.radio.univ-rennes1.fr>), should reduce need for liver biopsy, especially in patients presenting with unexplained hyperferritinaemia, without significant clinical and biochemical signs of liver disease.<sup>30</sup>

#### Contributors

Y Gandon designed and managed the study and wrote the report. D Oliu e acquired data at the study centre, and C Aub e did so at the validation centre. D Guyader, Y Deugnier, and F Oberti, enrolled patients and obtained data at the study and validation centres, respectively. V Sebill e was responsible for statistical analysis. Y Deugnier and V Sebill e helped to write the report. Y Gandon had full access to all data in the study and final responsibility to submit the report for publication. All authors have seen and approved the final version.

#### Conflict of interest statement

None declared.

#### Acknowledgments

We thank technical and professional staff of both magnetic resonance units for their help in undertaking this study, particularly Loic Sorel and Sam Nasser for doing masked measurements of magnetic resonance signal intensities; Christophe Gour for independent data management; and Eric Bellissant for help with statistical analysis. This work was supported by a grant from the Health Ministry of France (Projet Hospitalier de Recherche Clinique 1994) and by the Association Fer et Foie.

#### References

- Deugnier Y, Turlin B, Loreal O. Iron and neoplasia. *J Hepatol* 1998; **28**: 21–25.
- de Valk B, Marx JJ. Iron, atherosclerosis, and ischemic heart disease. *Arch Intern Med* 1999; **159**: 1542–48.
- Pawlotsky Y, Le Dantec P, Moirand R, et al. Elevated parathyroid hormone 44–68 and osteoarticular changes in patients with genetic hemochromatosis. *Arthritis Rheum* 1999; **42**: 799–806.
- Bonkovsky HL, Banner BF, Rothman AL. Iron and chronic viral hepatitis. *Hepatology* 1997; **25**: 759–68.
- Mendler MH, Turlin B, Moirand R, et al. Insulin resistance-associated hepatic iron overload. *Gastroenterology* 1999; **117**: 1155–63.
- Deugnier Y, Moirand R. Iron overload and public health. *Bull Acad Natl Med* 2000; **184**: 365–73.
- Brissot P, Deugnier Y. Haemochromatosis. In: McIntyre N, Benhamou JP, Bircher J, Rizzetto M, Rodes J, eds. Oxford textbook of clinical hepatology. Oxford: Oxford University Press, 1999: 1379–91.
- Barry M, Sherlock S. Measurement of liver-iron concentration in needle-biopsy specimens. *Lancet* 1971; **1**: 100–03.
- Guyader D, Gandon Y, Robert JY, et al. Magnetic resonance imaging and assessment of liver iron content in genetic hemochromatosis. *J Hepatol* 1992; **15**: 304–08.
- Guyader D, Gandon Y, Deugnier Y, et al. Evaluation of computed tomography in the assessment of liver iron overload: a study of 46 cases of idiopathic hemochromatosis. *Gastroenterology* 1989; **97**: 737–43.
- Brittenham GM, Farrell DE, Harris JW, et al. Magnetic-susceptibility measurement of human iron stores. *N Engl J Med* 1982; **307**: 1671–75.
- Gandon Y, Guyader D, Heautot JF, et al. Hemochromatosis: diagnosis and quantification of liver iron with gradient-echo MR imaging. *Radiology* 1994; **193**: 533–38.
- Ernst O, Sergent G, Bonvarlet P, Canva-Delcambre V, Paris JC, L'Hermine C. Hepatic iron overload: diagnosis and quantification with MR imaging. *Am J Roentgenol* 1997; **168**: 1205–08.
- Bonkovsky HL, Rubin RB, Cable EE, Davidoff A, Rijcken TH, Stark DD. Hepatic iron concentration: noninvasive estimation by means of MR imaging techniques. *Radiology* 1999; **212**: 227–34.

- 15 Poynard T, Bedossa P, Opolon P. Natural history of liver fibrosis progression in patients with chronic hepatitis C. *Lancet* 1997; **349**: 825–32.
- 16 Jensen JH and Chandra R. Theory of nonexponential NMR signal decay in liver with iron overload or superparamagnetic iron oxide particles. *Magn Reson Med* 2002; **47**: 1131–38.
- 17 Bland JM, Altman DG. Statistical methods for assessing agreement between two methods of clinical measurement. *Lancet* 1986; **1**: 307–10.
- 18 Stark DD. Hepatic iron overload: paramagnetic pathology. *Radiology* 1991; **179**: 333–35.
- 19 Rocchi E, Cassanelli M, Borghi A, et al. Magnetic resonance imaging and different levels of iron overload in chronic liver disease. *Hepatology* 1993; **17**: 997–1002.
- 20 Kaltwasser JP, Gottschalk R, Schalk KP, Hartl W. Non-invasive quantitation of liver iron-overload by magnetic resonance imaging. *Br J Haematol* 1990; **74**: 360–63.
- 21 Gomori JM, Horev G, Tamary H, et al. Hepatic iron overload: quantitative MR imaging. *Radiology* 1991; **179**: 367–69.
- 22 Hernandez RJ, Sarnaik SA, Lande I, et al. MR evaluation of liver iron overload. *J Comput Assist Tomogr* 1988; **12**: 91–94.
- 23 Fenzi A, Bortolazzi M, Marzola P. Comparison between signal-to-noise ratio, liver-to-muscle ratio, and  $1/T_2$  for the noninvasive assessment of liver iron content by MRI. *J. Magn Reson Imaging* 2003; **17**: 589–92.
- 24 Kreeftenberg HG Jr, Mooyaart EL, Huizenga JR, Sluiter WJ, Kreeftenberg HG. Quantification of liver iron concentration with magnetic resonance imaging by combining T1-, T2-weighted spin echo sequences and a gradient echo sequence. *Neth J Med* 2000; **56**: 133–37.
- 25 Villeneuve JP, Bilodeau M, Lepage R, Cote J, Lefebvre M. Variability in hepatic iron concentration measurement from needle-biopsy specimens. *J Hepatol* 1996; **25**: 172–77.
- 26 Outwater EK, Blasbalg R, Siegelman ES, Vala M. Detection of lipid in abdominal tissues with opposed-phase gradient-echo images at 1.5 T: techniques and diagnostic importance. *Radiographics* 1998; **18**: 1465–80.
- 27 Siegelman ES. MR imaging of diffuse liver disease: hepatic fat and iron. *Magn Reson Imaging Clin N Am* 1997; **5**: 347–65.
- 28 Gandon Y. Detection and quantification of liver iron overload using MRI: multicentric validation. Proceedings of the Radiological Society of North America. Nov 29–Dec 4, 1998; Chicago, IL, USA. Proceedings in Radiology: 209 (P).
- 29 Alustiza J. Quantification of hepatic iron concentration using magnetic resonance imaging. Proceedings of the Radiological Society of North America. Nov 26–Dec 1, 2000; Chicago, IL, USA. Proceedings in Radiology: 217 (P).
- 30 Guyader D, Jacquelinet C, Moirand R, et al. Noninvasive prediction of fibrosis in C282Y homozygous hemochromatosis. *Gastroenterology* 1998; **115**: 929–36.

## Uses of error

### Urine pregnancy test and intrauterine inseminations

Mahantesh A Karoshi

I recently learnt a lesson that I will never forget. A patient on infertility treatment underwent an intrauterine insemination (IUI) procedure. 2 weeks later she was admitted to the gynaecology ward with iliac fossa pain and a positive pregnancy test. Subsequently she underwent laparoscopic salpingectomy for an ectopic pregnancy. In this case we had not been sure whether she was pregnant at the time of IUI procedure. Therefore we decided that in future we would do a urine pregnancy test for all patients before IUI.

Later in the week we did a first patient's urine pregnancy test before IUI, and it was positive. Everyone was excited. The patient and her partner were congratulated and sent home without IUI. On the same day we did the same procedure for the second IUI

patient and again the pregnancy test was positive. However, this patient denied having had any sexual intercourse during the past 8 weeks. After evaluating her case notes and drug chart, we realised that she had received an injection of human chorionic gonadotropin (HCG) for ovulation 36 h previously. The positive pregnancy test we were witnessing was caused by the free fraction of the injected HCG being secreted in urine.

Therefore we changed our protocol again. Now, all patients have two urine pregnancy tests, one before they start ovulation induction treatment and one 12 days after IUI. The first patient was contacted, we explained why her urine pregnancy test had been positive, and she underwent IUI later that day.

Department of Obstetrics and Gynaecology, North Middlesex University Hospital, London N18 1QX, UK (M A Karoshi MD)